Polarization-Insensitive Single- and Broadband Switchable Absorber/Reflector and Its Realization Using a Novel Biasing Technique

Saptarshi Ghosh and Kumar Vaibhav Srivastava

***Abstract*— In this communication, a switchable absorber/reflector based on active frequency-selective surface (AFSS) has been presented for single- as well as broadband applications. The FSS comprises periodic patterns of square loops connected among themselves through p-i-n diodes, which exhibit switchable performances. The novelty of the proposed design lies in its symmetric configuration and biasing network, which makes the structure polarization insensitive unlike the earlier reported AFSSs. A single-band switchable absorber/reflector has initially been realized, which is characterized through an equivalent circuit model to derive the circuit parameters. Later, surface-mount resistors have been implemented in the design to realize a wideband switchable absorber/reflector aimed for C-band applications. Both the structures have used a novel biasing methodology to provide the bias voltage to semiconductor switches without disturbing the original resonance pattern. Furthermore, the fabricated samples, while measuring in an anechoic chamber, show good agreement with the simulated responses under normal incidence as well as for different polarization angles.**

***Index Terms*— Active frequency-selective surface (AFSS), broadband absorber, p-i-n diodes, switchable FSS.**

I. Introduction

Electromagnetic (EM) wave absorbers have manifold applications in different areas such as radar cross section, EM interference, and EM compatibility [1]–[3]. Conventional passive microwave absorbers such as Salisbury screen, Jaumann absorber use resistive sheets placed in front of a conducting plane to provide absorption at selected resonant frequencies [4], [5]. Later, the absorber technology based on frequency-selective surface (FSS) has been developed to reduce the bulky size and improve absorption performance [6]. Several methods such as multiple resonances, multilayer structures, lossy resistive sheet, and lumped resistors have been reported to increase the bandwidth of FSS-based absorbers [7]–[10]. Among them, the circuit analog absorber is an effective solution to the narrow-bandwidth problem, where chip resistors have been soldered on a metal patch printed on a grounded dielectric substrate.

Although the use of lumped resistors can increase the bandwidth of FSS absorbers, they remain passive structures with fixed reflectivity characteristics. A passive FSS might be considered to have limited applications, as it offers no flexibility once fabricated, whereas an active FSS (AFSS) has reconfigurable properties due to the presence of external control [11], [12]. The AFSS-based absorbers can be used for tuning applications where the absorption bandwidth can be regulated to desired frequency band [13]–[15]. Switchable AFSS absorber/reflector is another important application, where the absorption can be switched ON/OFF at the frequency of interest by applying some external stimuli, usually a biasing circuit. They can be used in stealth systems, where the incident EM wave is absorbed to hide the object in absorptive state, and it works as a perfect reflector in complementary state [16]. Another application where switchable absorber/reflector can be used is the area of compressive imaging, where an array of switchable reflectors can be used to form frequency-selective spatial light modulators [17].

In the past few years, several switchable absorber/reflector designs have been reported in the literature [18]–[21]. Zhu *et al.* [18] and Xu and Sonkusale [19] have developed single-band absorbers/reflectors using switchable properties, where an active semiconductor switch (p-i-n diode) has been embedded between the unit cells. Since the diodes are present between the unit cells in a particular direction, the structures exhibit switchable operation only for a specific polarization. In [20], a switchable absorber has been designed for two opposite polarizations where the biasing network has been supplied through vias. A broadband FSS absorber/reflector has been reported recently for a single polarization [21]. However, all these designs suffer from polarization-sensitive behavior, which is quite undesirable for many EM applications. Since the biasing network of AFSS-based polarization-insensitive absorbers has to be carefully isolated under different polarizations of incident waves, active polarization-insensitive absorbers are more difficult to be accomplished compared with passive polarization-independent absorbers.

In this communication, a single-band switchable absorber/reflector has been designed based on AFSS and the concept has been extended to realize another switchable wideband absorber. Both the structures offer two advantages compared with all the previously reported AFSS structures.

1) The designs are fourfold symmetric and therefore offer switchable characteristics for all polarization angles.
2) A novel biasing network has been designed to provide bias voltage to all the semiconductor switches without disturbing the structure resonance.

The single-band structure, introduced in Section II, is based on square loops and switches at a single resonant frequency. The broadband structure, described in Section III, has the lumped resistors implemented on the square loops patterned on a dielectric substrate. Furthermore, good agreement between the simulated and measured responses validates the reconfigurability of both the designs for different polarization angles under normal incidence.

II. Single-Band Switchable Absorber/Reflector

A. Design and Analysis

A square loop is a well-known FSS element geometry comprising polarization insensitivity and good angular stability performance. The FSS structure typically resonates at a particular frequency where the wavelength is comparable to the perimeter size.

An active absorber has been designed by the periodic square loops imprinted on a grounded dielectric substrate. Each of the loops is connected with four other square loops through semiconductor switches along the diagonals. Fig. 1(a) and (b) illustrate the array structure and unit cell geometry, respectively, of the proposed switchable single-band absorber. The top and bottom metal patches are made of copper with a conductivity (σ) of 5.8×10^7 S/m and a thickness of 0.035 mm, whereas FR4 is used as the intermediate dielectric substrate having a relative permittivity (ε_r) of 4.4 and a loss tangent ($\tan\delta$) of 0.02. The switches chosen are BAP 70-03 silicon p-i-n diodes from NXP with an equivalent forward resistance in ON state and an equivalent capacitance in OFF state. In both the states, an equivalent series inductance has also been considered as given in data sheet [22].

When the structure is excited by a plane EM wave, each square loop element exhibits an equivalent inductance (L) along the direction of the incident electric field and an equivalent resistance (R) due to finite conductivity of the metal strip. When the diode is in ON state under forward bias voltage, it provides a low resistance.

Manuscript received January 11, 2016; revised April 20, 2016; accepted April 21, 2016. Date of publication May 10, 2016; date of current version August 2, 2016. This work was supported in part by ISRO, India under Project No. SPO/STC/EE/2014087. *(Corresponding author: Saptarshi Ghosh.)*

The authors are with the Department of Electrical Engineering, IIT Kanpur, Kanpur 208016, India (e-mail: joysaptarshi@gmail.com; kvs@iitk.ac.in).

Color versions of one or more of the figures in this communication are available online at http://ieeexplore.ieee.org.

Digital Object Identifier 10.1109/TAP.2016.2565720

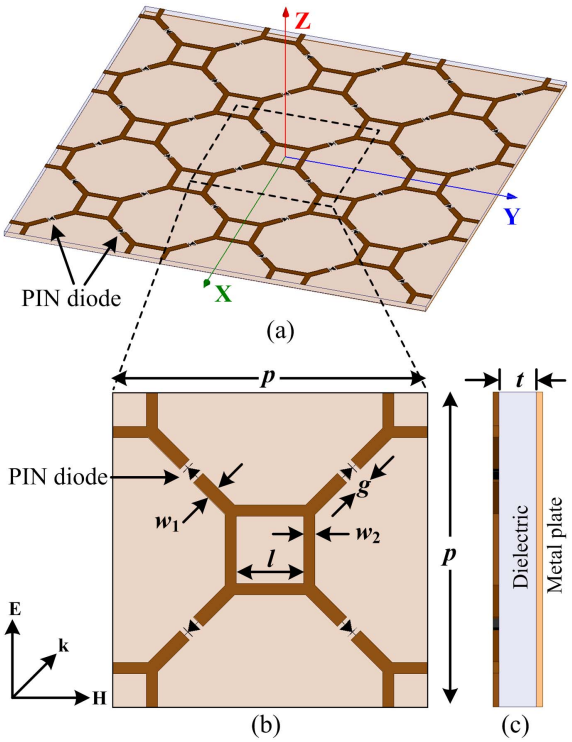

Fig. 1. Geometry of the proposed switchable single-band absorber/reflector. (a) Perspective view. (b) Top and (c) side views of the unit cell structure. The optimized geometrical dimensions are: $p = 28$ mm, $l = 6$ mm, $w_1 = 1.2$ mm, $w_2 = 1$ mm, $g = 1.7$ mm, and $t = 1$ mm.

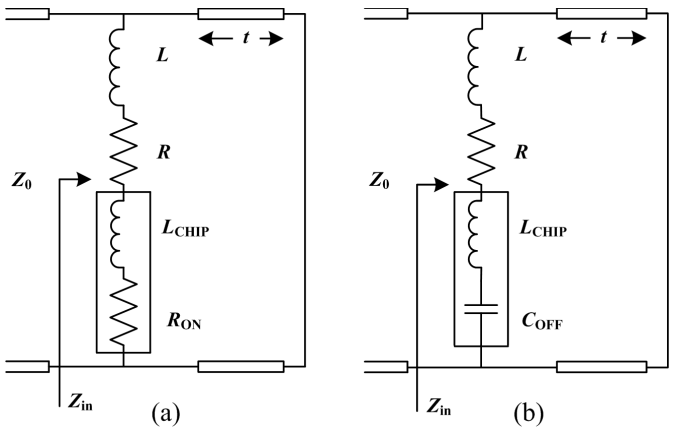

Fig. 2. Equivalent circuit model of the proposed switchable single-band structure in (a) ON state and (b) OFF state.

Then the diagonal copper strips, connected between the consecutive square loops, behave as short circuits. Thus, the structure does not generate any resonance due to the absence of any equivalent capacitance at the top surface and therefore realizes as a perfect reflector over a wide frequency range. Fig. 2(a) shows the equivalent circuit model of the structure in ON state which consists of a square loop inductance (L) and resistance (R), a chip inductance (L_{CHIP}), and a small diode resistance (R_{ON}).

Under reverse bias, the diode is in OFF state with a large capacitive impedance (C_{OFF}) and therefore, the diagonal strips exhibit an equivalent capacitance as observed from Fig. 2(b). Then the FSS structure, having an equivalent inductance and capacitance, resonates at a particular frequency which results in a perfect absorption in OFF state.

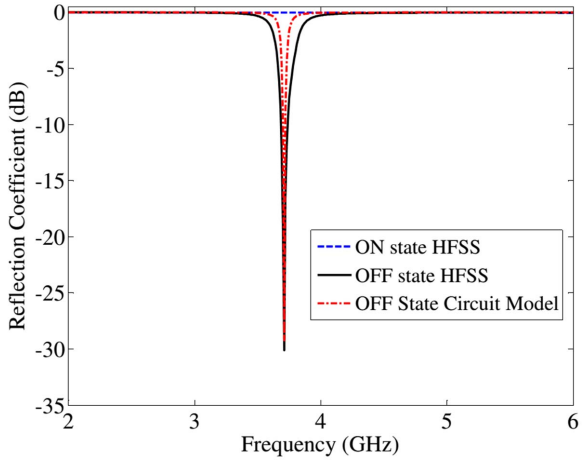

Fig. 3. Reflectivity of the single-band switchable structure calculated from the equivalent circuit model in OFF state and simulated using HFSS under normal incidence for both ON and OFF states.

In order to validate the equivalent circuit model of the single-band switchable absorber in OFF state, the reflectivity performance obtained from the circuit model and full wave simulation has been compared as shown in Fig. 3. The values of lumped elements are determined as: $L = 57.26$ nH and $R = 10.26\ \Omega$, whereas the diode parasitic components are extracted from data sheet as: $L_{\text{CHIP}} = 1.5$ nH and $C_{\text{OFF}} = 0.1$ pF. Fig. 3 shows the simulated reflectance of the proposed structure using Finite Element Method-based full-wave simulator High Frequency Structure Simulator (HFSS) under normal incidence. In OFF state, the structure exhibits a single absorption peak at 3.71 GHz with reflection coefficient of -30.08 dB, while in ON state the FSS has nearly perfect reflective characteristic over the frequency range.

The novelty of the proposed structure lies in its symmetrical design as observed from Fig. 1. Since the structure is fourfold symmetric, it will exhibit similar reflection performance for all the polarization angles and therefore can be considered as a polarization-insensitive structure. The biasing networks applied across the p-i-n diodes have no considerable effect on the design symmetry as discussed in detail in Section II-B.

The proposed structure has also been studied for oblique incidence as shown in Fig. 4. The structure shows good angular stability upto 45° incident angle for both TE and TM polarizations. With higher angle of incidence, the reflectivity gradually decreases in case of TE polarization, although remaining satisfactory for TM polarized wave. There is a small frequency shift (0.04 and 0.06 GHz for TE and TM polarized waves, respectively) with higher incident angles; however, all the reflection dips are observed within a common -10-dB bandwidth of 10 MHz (3.68–3.78 GHz).

B. Fabrication and Measurement

Since the biasing networks are to be provided in reconfigurable structures, it is very difficult to design a symmetrical FSS having unit cells arranged in periodic pattern. Although the biasing network needs not to be considered in the simulation, the fabricated structure has to incorporate the biasing lines such that the characteristic of the structure remains unaffected for different polarizations of incident waves. Simultaneously, the biasing lines should be isolated properly from the unit cell topology; otherwise, it will impact on the structure original performance. Inductors of correct values can be used for the required isolation.

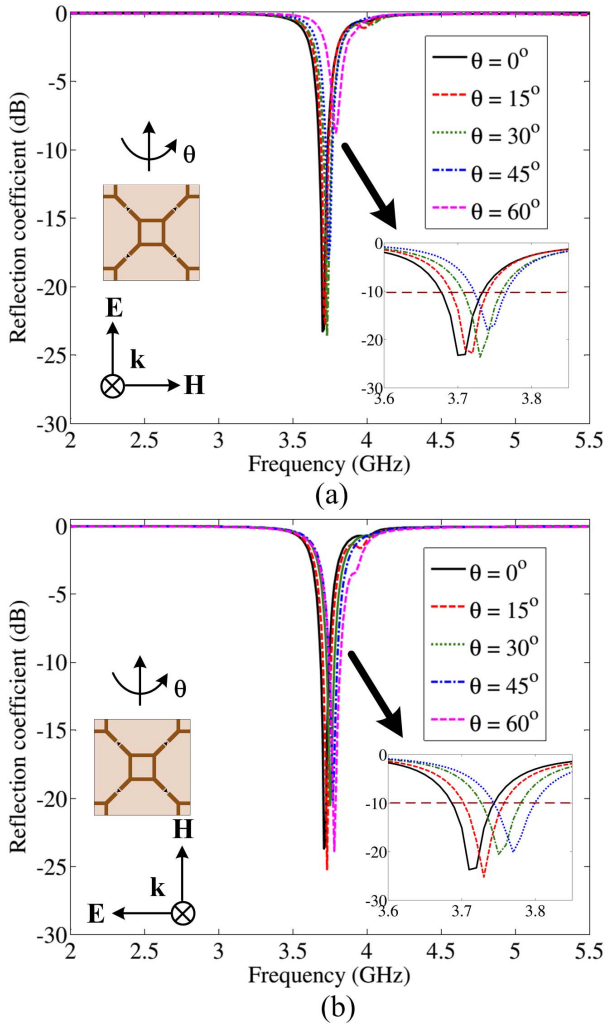

Fig. 4. Simulated reflection coefficients for different incident angles under (a) TE and (b) TM polarizations of the single-band switchable absorber. Inset: −10-dB bandwidth under oblique incidence of the proposed structure.

Initially, the square loop array structure has been fabricated on the top surface of a 1-mm-thick FR4 sheet whose back side is completely metal laminated. The geometrical dimensions of the structure are depicted in Fig. 1. The overall size of the sample is 140 mm × 140 mm, on which 41 square loops are printed. BAP 70-03 p-i-n diodes are soldered on the fabricated sample using surface-mount technology, which work as a low resistance at forward voltage and large capacitance at reverse voltage.

In order to provide the biasing network, two biasing lines are printed at the two sides of the sample as shown in Fig. 5. Square loops present in the odd rows are connected to the right-sided biasing line, whereas the left-sided biasing line is attached with the loops in the even rows. The diodes connected to the square loops are in outward direction for one row, while in inward direction for the next row [as shown in Fig. 1(b)]. HK 1005 series of inductors from TAIYO YUDEN are used between the successive metal loops to achieve the required isolation as well as to protect the biasing lines from alternating signal. The inductor has a value of 12 nH, which has a self-resonating frequency of 3.62 GHz, and therefore can provide required isolation near the absorption frequency 3.71 GHz.

The cathodes and the anodes of all the p-i-n diodes are joined with the square loops attached with the left- and right-sided biasing line, respectively. Therefore, when the right and left biasing lines are connected with the positive and negative ends of the supply voltages,

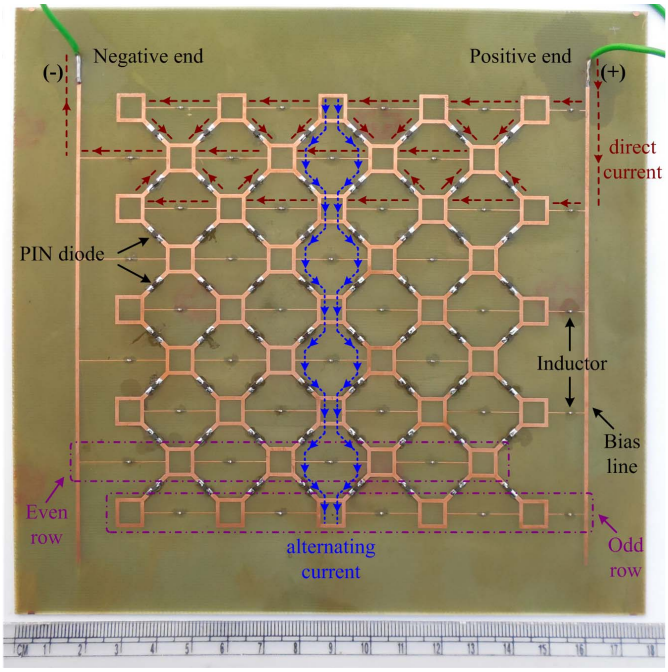

Fig. 5. Picture of the fabricated switchable single-band structure. The arrow directions show the flow of current through the sample in ON state.

respectively, direct current will flow through the p-i-n diodes and inductors, as observed by red dotted lines from Fig. 5. In a similar way, alternating current will flow through the square loops and p-i-n diodes uninterruptedly in the direction of the electric field as illustrated by blue dotted lines in Fig. 5. It is clearly understood that there will be no equivalent capacitance at the top surface in the structure when the diodes are in ON state. This will provide perfect reflection behavior due to absence of any resonance frequency. On the contrary, when the diodes are biased with zero or negative supply voltage, high-capacitive impedance will be generated across the diodes and the fabricated sample will show a single absorption at a particular frequency. In both the states, the biasing network will not affect the absorption/reflection characteristic. Furthermore, this biasing technique uses all the p-i-n diodes in parallel connection unlike the earlier reported AFSS designs where the switches are connected in series. This reduces the overall bias voltage compared with the previous ones as well as protects the switches from damage.

In order to perform the experiment, a pair of horn antennas is used to measure the reflection from the fabricated structure. One of the antennas acts as a transmitter and another antenna behaves as a receiver and both the antennas are connected with an Agilent N5230A network analyzer. The whole setup is placed inside an anechoic chamber and the measurement is performed using the free space technique [23].

The reflectivities of the fabricated sample in ON and OFF states under normal incidence have been compared with the simulated responses as shown in Fig. 6(a). In OFF state, the structure has a perfect absorption at 3.70 GHz with reflection coefficient of −19.1 dB, whereas complete reflection is observed during ON state. A slight deviation between the simulated and measured results is observed, which may be due to small error in p-i-n diode parasitic values and fabrication tolerance.

In order to verify the polarization-insensitive behavior of the switchable absorber/reflector, the reflection coefficients under OFF state are measured by rotating the fabricated structure around its axis from 0° to 45° in steps of 15°, and the measured response is

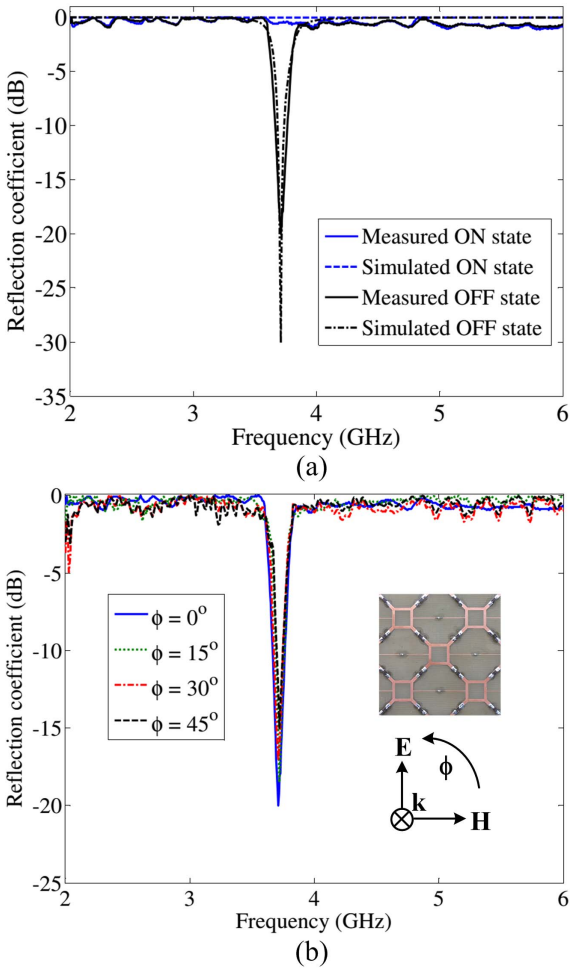

Fig. 6. (a) Comparison of simulated and measured reflection coefficients under normal incidence. (b) Measured reflection coefficients for different polarization angles under normal incidence of the single-band structure.

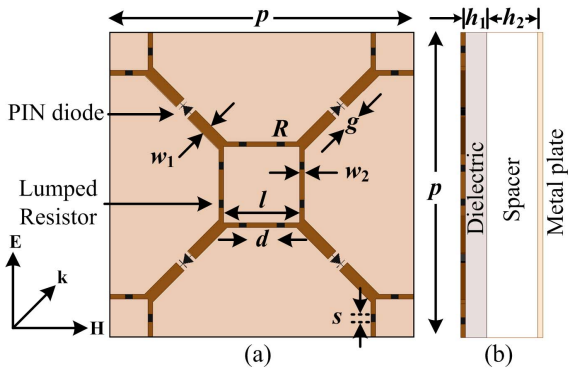

Fig. 7. Unit-cell geometry of the proposed switchable broadband absorber/reflector. (a) Top and (b) side views of the unit cell structure.

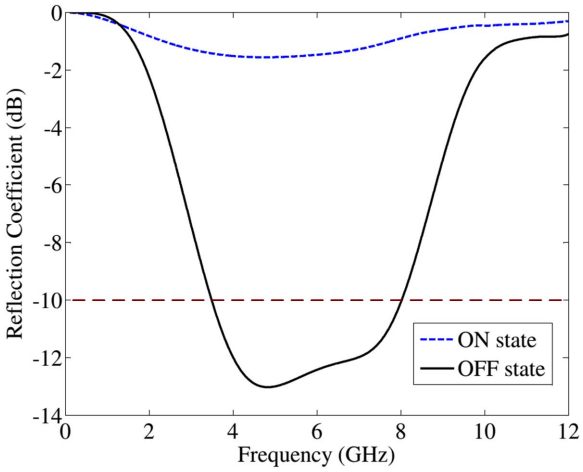

Fig. 8. Reflectivity of the switchable broadband absorber for ON and OFF states under normal incidence.

shown in Fig. 6(b). It is observed that the reflection dips almost coincide for all polarization angles, which validates that the absorber is polarization insensitive. The measurement also shows that the biasing methodology does not affect the polarization-insensitive characteristic of the fabricated sample.

III. Broadband Switchable Absorber/Reflector

A. Design and Analysis

In order to extend the absorption bandwidth of the proposed switchable polarization-insensitive absorber, the design has further been modified by incorporating lumped resistors in the square loops. The dimensions of the unit cell geometry has also been changed to optimize the absorption bandwidth aimed at C-band (4–8 GHz), which is one of the most important frequency bands in microwave application.

The FSS is loaded with surface-mount resistors in the arms of the square loops and each of the loops is connected with four other square loops through p-i-n diode as illustrated in Fig. 7. The same FR4 dielectric is used to print the metallic pattern, whereas an air spacer has been used between the dielectric and bottom metal ground. The geometric dimensions of the broadband structure are optimized as: $p = 32$ mm, $l = 8$ mm, $w_1 = 1.2$ mm, $w_2 = 0.5$ mm, $g = 1.7$ mm, $d = 3.2$ mm, $s = 0.8$ mm, $R = 120\ \Omega$, $h_1 = 1$ mm, and $h_2 = 8$ mm.

When the structure is simulated in the HFSS software, it is observed from Fig. 8 that the reflection coefficient is less than -10 dB over the frequency range of 3.48–8.04 GHz, which is 79.17% at 5.76 GHz in OFF state. However, in ON state, the proposed structure has good reflectance performance (max reflection coefficient of -1.56 dB) over the entire C-band frequency range. The reflection is not exactly perfect (unlike that of the single-band switchable structure) due to the presence of lumped resistors, which obstruct the path of alternating current and resulting in ohmic loss.

As observed from Fig. 7, the structure retains its fourfold symmetric design and therefore maintains polarization-insensitive behavior. The broadband structure has also been studied under oblique incidence for both TE and TM polarizations in OFF state as observed from Fig. 9. In case of TE polarization, the absorption bandwidth shifts to a higher frequency range, whereas the -10-dB bandwidth reduces to 2.8 GHz (4.08–6.88 GHz) at 30° angle of incidence for TM polarized wave. With higher incident angles, the structure absorptivity gradually reduces, thereby maintaining angular stability upto 15° and 30° angles of incidence for TE and TM polarized waves, respectively.

B. Experimental Verification

In order to experimentally validate the switchable broadband structure, the structure has been fabricated using printed circuit board technology in a similar way described in Section II. The p-i-n diodes and the biasing lines have also been implemented similarly. Chip resistors of 120 Ω (2RKF1200X) from Panasonic are soldered on the sample using surface-mount technology. The overall size of the fabricated structure is 128 mm × 128 mm, on which 41 square loops are printed and a total of 328 chip resistors are

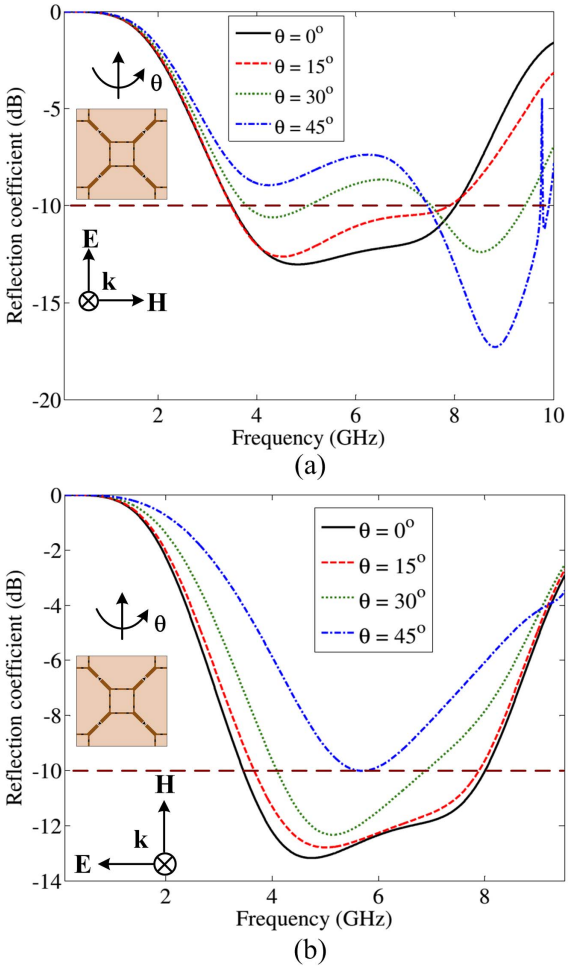

Fig. 9. Simulated reflection coefficients for different incident angles under (a) TE and (b) TM polarizations of the proposed switchable broadband structure in OFF state.

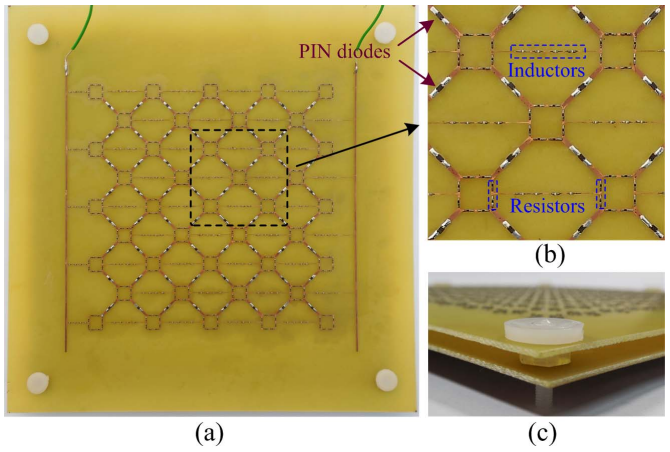

Fig. 10. Picture of the fabricated switchable broadband structure. (a) Complete view and (b) enlarged view of top layer. (c) Air spacer supported by plastic nut and bolt.

soldered as shown in Fig. 10(a). In order to maintain an 8-mm air gap between the dielectric substrate and the ground plane, plastic nuts and bolts are used at the four corners of the structure. The air gap can also be realized using a commercially available foam material HF-51 from ROHACELL having air-like properties and a

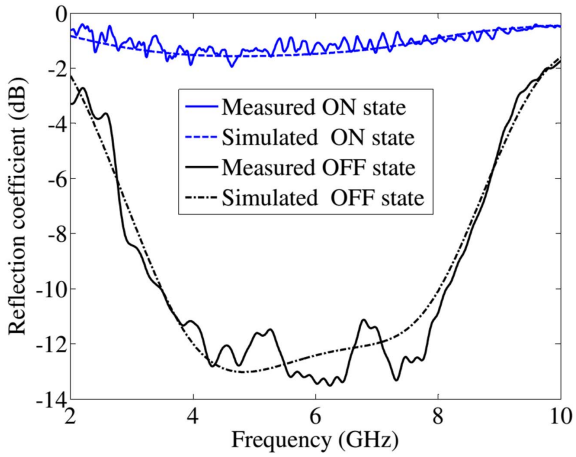

Fig. 11. Comparison of simulated and measured reflection coefficients under normal incidence of the broadband switchable structure.

dielectric constant of 1.05 without affecting the absorption performance. The enlarged view of the unit cell and the air spacer are illustrated in Fig. 10(b) and (c), respectively.

Another modification in the fabricated sample compared with the single-band structure is that the use of multiple-valued inductors. Since the commonly used inductors are of narrow band in nature, and the biasing lines have to be isolated from the resonant patterns for the entire *C*-band frequency range, we have chosen a series of inductors having successive self-resonating frequencies. In order to attain a 4–8 GHz isolation, four HK 1005 series of inductors with values of 3, 3.9, 5.6, and 8.2 nH (from Taiyo Yuden) have been connected in series, so that the overall impedance response of the biasing line has wideband characteristics in the required frequency band.

The fabricated structure along with the entire setup is placed inside an anechoic chamber and the measurement has been carried out using the free-space technique. Fig. 11 shows the comparison between the simulated and measured responses of the broadband switchable structure under normal incidence for both ON and OFF states. In case of OFF state, the measured result shows a 10-dB absorption bandwidth of 4.66 GHz (3.56–8.16 GHz) having a percentage bandwidth of 79.52% at 5.86 GHz, whereas the structure exhibits good reflection performance in the entire frequency range for ON state.

IV. Conclusion

In this communication, a switchable absorber/reflector based on AFSS has been reported for single-band as well as wideband applications. The novelty of the design lies in its fourfold symmetry, which makes the structure insensitive to all polarizations of incident wave unlike the earlier AFSSs. A biasing network has also been designed to perform the measurement of the proposed structures, which shows good agreement between the simulated and measured responses. This biasing method offers two advantages over the earlier ones.

1) The alternating and direct current paths are different enabling independent tuning of the structures.
2) It uses p-i-n diodes in parallel connection rather than series along with proper isolation by correct-valued inductors.

Therefore, this biasing network can be implemented to any symmetrical AFSSs for experimental verification without further disturbing the original resonance pattern. In addition, the proposed structures have the advantages of simplified geometry, angular stability, as well as single-band and wideband characteristics compared with previously reported switchable absorbers/reflectors.

ACKNOWLEDGMENT

The authors want to thank P. Chongder for his valuable suggestion, and V. Kumar Singh and S. Pramanik for their help fabricating the structures.

REFERENCES

[1] A. Fallahi, A. Yahaghi, H. R. Benedickter, H. Abiri, M. Shahabadi, and C. Hafner, "Thin wideband radar absorbers," *IEEE Trans. Antennas Propag.*, vol. 58, no. 12, pp. 4051–4058, Dec. 2010.

[2] N. Ono, Y. Hayashi, A. Kisuki, and Y. Ikeda, "Anechoic chamber and wave absorber," U.S. Patent EP 0 660 123 A2, Jun. 28, 1995.

[3] K. J. Vinoy and R. M. Jha, *Radar Absorbing Materials: From Theory to Design and Characterization*, 1st ed. Norwell, MA, USA: Kluwer, 1996.

[4] R. L. Fante and M. T. McCormack, "Reflection properties of the Salisbury screen," *IEEE Trans. Antennas Propag.*, vol. 36, no. 10, pp. 1443–1454, Oct. 1988.

[5] E. F. Knott, J. F. Schaeffer, and M. T. Tulley, *Radar Cross Section*, 2nd ed. Raleigh, NC, USA: SciTech, 2004.

[6] B. A. Munk, *Frequency Selective Surfaces: Theory and Design*, 1st ed. New York, NY, USA: Wiley, 2000.

[7] J. Lee and S. Lim, "Bandwidth-enhanced and polarisation-insensitive metamaterial absorber using double resonance," *Electron. Lett.*, vol. 47, no. 1, pp. 8–9, Jan. 2011.

[8] S. Ghosh, S. Bhattacharyya, D. Chaurasiya, and K. V. Srivastava, "Polarisation-insensitive and wide-angle multi-layer metamaterial absorber with variable bandwidths," *Electron. Lett.*, vol. 51, no. 14, pp. 1050–1052, Jul. 2015.

[9] F. Costa, A. Monorchio, and G. Manara, "Analysis and design of ultra thin electromagnetic absorbers comprising resistively loaded high impedance surfaces," *IEEE Trans. Antennas Propag.*, vol. 58, no. 5, pp. 1551–1558, May 2010.

[10] Y. Shang, Z. Shen, and S. Xiao, "On the design of single-layer circuit analog absorber using double-square-loop array," *IEEE Trans. Antennas Propag.*, vol. 61, no. 12, pp. 6022–6029, Dec. 2013.

[11] P. S. Taylor, E. A. Parker, and J. C. Batchelor, "An active annular ring frequency selective surface," *IEEE Trans. Antennas Propag.*, vol. 59, no. 9, pp. 3265–3271, Sep. 2011.

[12] B. Sanz-Izquierdo and E. A. Parker, "Dual polarized reconfigurable frequency selective surfaces," *IEEE Trans. Antennas Propag.*, vol. 62, no. 2, pp. 764–771, Feb. 2014.

[13] A. Tennant and B. Chambers, "A single-layer tuneable microwave absorber using an active FSS," *IEEE Microw. Wireless Compon. Lett.*, vol. 14, no. 1, pp. 46–47, Jan. 2004.

[14] B. Xu, C. Gu, Z. Li, L. Liu, and Z. Niu, "A novel absorber with tunable bandwidth based on graphene," *IEEE Antennas Wireless Propag. Lett.*, vol. 13, pp. 822–825, May 2014.

[15] J. Li *et al.*, "Design of a tunable low-frequency and broadband radar absorber based on active frequency selective surface," *IEEE Antennas Wireless Propag. Lett.*, vol. 15, pp. 774–777, Mar. 2016.

[16] W. F. Bahret, "The beginnings of stealth technology," *IEEE Trans. Aerosp. Electron. Syst.*, vol. 29, no. 4, pp. 1377–1385, Oct. 1993.

[17] D. Shrekenhamer, C. M. Watts, and W. J. Padilla, "Terahertz single pixel imaging with an optically controlled dynamic spatial light modulator," *Opt. Exp.*, vol. 21, no. 10, pp. 12507–12518, May 2013.

[18] B. Zhu, C. Huang, Y. Feng, J. Zhao, and T. Jiang, "Dual band switchable metamaterial electromagnetic absorber," *Prog. Electromagn. Res. B*, vol. 24, pp. 121–129, Aug. 2010.

[19] W. Xu and S. Sonkusale, "Microwave diode switchable metamaterial reflector/absorber," *Appl. Phys. Lett.*, vol. 103, p. 031902, Jul. 2013.

[20] B. Zhu, Y. J. Feng, J. M. Zhao, C. Huang, and T. Jiang, "Switchable metamaterial reflector/absorber for different polarized electromagnetic waves," *Appl. Phys. Lett.*, vol. 97, no. 5, p. 051906, Aug. 2010.

[21] P. Kong, X. W. Yu, M. Y. Zhao, Y. He, L. Miao, and J. J. Jiang, "Switchable frequency selective surfaces absorber/reflector for wide-band applications," *J. Electromag. Waves Appl.*, vol. 29, no. 11, pp. 1473–1485, May 2015.

[22] Accessed on Nov. 2015. [Online]. Available: http://www.nxp.com/documents/data_sheet/BAP70-03.pdf

[23] D. Ye *et al.*, "Towards experimental perfectly-matched layers with ultra-thin metamaterial surfaces," *IEEE Trans. Antennas Propag.*, vol. 60, no. 11, pp. 5164–5172, Nov. 2012.

On the Treatment of Arbitrary Boundary Conditions Using a Fast Direct $\mathcal{H}$-Matrix Solver in MoM

Alexander Vogt, Torsten Reuschel, Heinz-D. Brüns, Sabine Le Borne, and Christian Schuster

***Abstract*— This communication adapts the formalism of hierarchical ($\mathcal{H}$-) matrices to the direct solution process (LU decomposition) of the method of moments (MoM) in the frequency domain. A novel clustering approach based on physical constraints is presented and extended to treat dielectric bodies as well as arbitrary boundary conditions. Comparisons with other numerical methods are provided. The analyses show a considerable speedup of the computation times and a significant reduction of required memory compared with the traditional MoM solution process, especially for highly resonant structures where iterative solvers like the multilevel fast multipole algorithm show poor convergence.**

***Index Terms*— Boundary conditions, direct solver, hierarchical ($\mathcal{H}$-) matrices, integral equations, method of moments (MoM).**

I. INTRODUCTION

The method of moments (MoM) [1] is well known as a general purpose full-wave numerical method that requires fully populated system matrices. This leads to a considerable computational effort if the number of unknowns increases. Especially for electrically large structures or geometrically detailed geometries, this poses a limit on the applicability of MoM solvers. Fast iterative solvers accelerated by the multilevel fast multipole algorithm (MLFMA) [2], or based on kernel-independent algebraic methods [3], such as the Integral Equation QR solver [4], [5] or the Multilevel Matrix Decomposition Algorithm (MLMDA) [6], have been developed to reduce both the memory consumption and the simulation time. However, these solvers often exhibit slow convergence if resonant structures are present. In addition, the multipole methods require that the object dimensions are in the order of the considered wavelength or larger without low-frequency stabilization. This effectively sets a lower frequency limit. In addition, solving a problem with multiple right-hand sides (RHSs) requires an individual solution process for each of the excitation vectors. This is often encountered in the calculations of radar cross sections or if multiple ports are present in the system.

To overcome these issues, focus has been put on fast direct solvers. These include techniques, such as the MLMDA [7]–[9], adaptive cross approximation (ACA)-based solvers [10], [11], and hierarchical ($\mathcal{H}$-) matrix solvers. Recently, the latter has gathered much attention in various topics of computational electromagnetics (CEM) such as the 2-D boundary element method [6], the 3-D MoM [10], [12], [13], the quasi-static finite-element method (FEM) [14], the impedance extraction [15], and the study of planar layered structures [16]. However, in the context of the MoM, the references only consider the simple case with electric surface currents and a single type of boundary condition.

This communication extends the $\mathcal{H}$-matrix approach to treat dielectric bodies [17] and arbitrary boundary conditions such as perfect electrically conducting (PEC) and dielectric interfaces, or the thin sheet approximation [18]. Due to the respective underlying

Manuscript received January 29, 2015; revised April 23, 2016; accepted May 5, 2016. Date of publication May 19, 2016; date of current version August 2, 2016.

The authors are with the Technische Universität Hamburg–Harburg, 21079 Hamburg, Germany (e-mail: alexander.vogt@tuhh.de; torsten.reuschel@tuhh.de; bruens@tuhh.de; leborne@tuhh.de; schuster@tuhh.de).

Color versions of one or more of the figures in this communication are available online at http://ieeexplore.ieee.org.

Digital Object Identifier 10.1109/TAP.2016.2570803